Environmental Earth Sciences (2026) 85:58
https://doi.org/10.1007/s12665-025-12654-x

ORIGINAL ARTICLE

Heavy metals in perlite quarries and exposure of worker

Şeref Turhan[1] · Savaş Türkdoğan[2] · Ergin Murat Altuner[3] · Aslı Kurnaz[1] · Aybaba Hançerlioğulları[1]

Received: 27 May 2025 / Accepted: 11 October 2025 / Published online: 13 January 2026

Abstract

Heavy metal(loids) (HMs), which can be carcinogenic, cytotoxic, and mutagenic, can pose a threat to fauna, flora, and humans. In the mining industry, large amounts of HMs released uncontrolled as a result of activities such as extraction, grinding, clustering of mineral ores, and dumping of wastes in open areas. Perlite is a naturally occurring glassy volcanic alumina silicate rock that is mined and used all over the world. Perlite is utilized in the construction, agriculture, food, pharmaceutical, and chemical industries. This study focuses, for the first time, on the determination of HM contents of perlites produced as a result of mining in Türkiye and the assessment of potential health risks (PHRs) arising from HMs for quarry workers. The concentrations of HMs in 126 perlites samples collected from 12 quarries located in different geographical regions of Türkiye were analyzed by an energy-dispersive X-ray fluorescence (EDXRF) spectroscopy. The hazard index (HI) and total carcinogenic risk (TCR) index were estimated to assess non-carcinogenic and carcinogenic PHR for workers via three exposure pathways. The average concentrations of HMs analyzed in perlites samples were 4.2 (As), 4.3 (Cu), 7.0 (Co), 7.1 (V), 19.8 (Ni), 26.4 (Pb), 31.1 (Zn), 64.9 (Cr), 93.7 (Zr), 383.5 (Mn), 528.3 (Ti) and 6585.4 (Fe) mg kg^{-1} dw, which were below the upper continental crust average, exception for Pb. All HI and TCR values revealed that the non-carcinogenic and carcinogenic PHRs for adult quarry workers exposed to all HMs in the studied perlites were in the acceptable range.

Keywords Perlite · Heavy metals · Health risk assessment · EDXRF · Türkiye

Introduction

Although there is no consensus yet on the definition of the 'heavy metal' term (abbreviated as HM), it is generally used to refer to metallic and metalloid chemical elements that have a relatively high density or atomic weight compared to water density of 5 g/m^3 [1–5]. HMs are naturally found in the Earth's crust and well-known environmental contaminants. They can harm flora, fauna, ecosystems (terrestrial and aquatic), and humans due to their potential toxicity, non-biodegradability, persistence, and bioaccumulation, and irreversible properties [2, 6]. Therefore, HM pollution will inevitably pose a danger and threat to human health, food security, the ecosystem, and the global environment [2, 3, 6–9]. The toxicity of HMs, which can bring about various health problems as carcinogenic and non-carcinogenic, depends on different factors such as the chemical species, oxidation state, concentration of HM concerned, dose and route of exposure, and genetics, gender, age and nutritional status of exposed individuals [1, 7]. The most dangerous HMs for human and environmental health include chromium (Cr (VI)), arsenic (As), mercury (Hg), lead (Pb), cadmium (Cd), and nickel (Ni) [45]. These HMs are regarded as systemic toxicants that induce multiple organ damage even at lower exposure levels and are classified as known or probable human carcinogens [1]. However, some HMs such as Cr (III), zinc (Zn), copper (Cu), iron (Fe), and manganese (Mn) can be essential for living organisms and may be required in very low concentrations in the human body [2]. The HMs causing the environmental pollution in question can originate from lithogenic processes (volcanic activity, soil erosion, weathering of metal-bearing rocks, sediment resuspension, metal evaporation, etc.) and anthropogenic (mining, energy,

✉ Şeref Turhan
serefturhan63@gmail.com; sturhan@kastamonu.edu.tr

[1] Department of Physics, Faculty of Science, Kastamonu University, Kuzeykent, Kastamonu 37150, Türkiye

[2] Department of Physics, Institute of Science, Kastamonu University, Kuzeykent, Kastamonu 37150, Türkiye

[3] Department of Biology, Faculty of Science, Kastamonu University, Kuzeykent, Kastamonu 37150, Türkiye

industrial and agricultural processes, etc.) activities [2, 3]. The mining industry serves as one of the most important sectors of global technological and economic progress due to the provision of indispensable raw materials (minerals) for various industries or sectors [10]. However, the large quantities of HMs generated during the extraction, separation and processing operations of these mineral ores and the storage and disposal of wastes pose significant environmental hazards such as soil and water pollution and degradation of ecosystems [4, 9–15]. Therefore, the mining industry is considered a prime source of HM pollution in environments [4, 10].

The naturally occurring perlite is an amorphous volcanic alumino-silicate rock that is mined and used around the world [16–19]. When heated to 1100 °C, perlite converts natural water (2–5% of total weight) into vapor and becomes expansive and porous, expanding up to twenty times its original volume [16–19]. Expanded perlite has several attractive physical properties for commercial applications, such as high surface area, low thermal conductivity, high heat resistance, low sound transmission, and chemical inertness [17]. Because of these properties, expanded perlites are used in the construction, agriculture, food, pharmaceutical, and chemical industries [17]. The vast majority of perlites are used in the construction industry, particularly in the production of cement and bricks for ceiling tiles and roof insulation products. Perlites are an important commodity in the horticulture industry, where they are mixed with soil. The addition of perlite to the soil increases the amount of water and oxygen held in the soil. perlite reserves in the world are concentrated in Tertiary-Early Middle Quaternary volcanic regions [20]. Perlites are generally extracted by open pit mining methods in various countries of the world, usually by blasting and/or dismantling (breaking with a bulldozer-toothed connection) [17, 20]. Raw perlite processing includes crushing, grinding, drying, screening, and sizing processes, and therefore, no chemicals are used in the processing of perlite [17]. USA, Armenia, Japan, Italy, Türkiye, and Greece are countries rich in perlite resources [17]. Türkiye's total possible perlite reserve is 4.5 billion tons [20]. Studies on perlites have generally focused on the use of expanded perlites in the construction industry and their performance as adsorbents for HMs in industrial wastes [18, 21–29].

According to our literature research, there is no detailed study on the determination of the HMs in perlites. The main motivation for this research is the necessity to determine the HMs that perlite, considering the use of perlites in various consumer products in different sectors and the occupational exposure of quarry workers to HMs. The objectives of this study are to determine the spatial distributions of HMs in commercially operated perlite quarries (PERQs) using an energy-dispersive X-ray fluorescence (EDXRF) spectroscopy and to assess the carcinogenic and non-carcinogenic potential human health risks (PHRs) that PERQ workers may be exposed to through accidental ingestion, inhalation, and dermal (skin) contact using the PHR evaluation method introduced by the United States Environmental Protection Agency (USEPA).

Materials and methods

Sample preparation

Türkiye's perlite reserves are around 4.5 billion tons, which constitutes a significant portion of the estimated world reserves [20]. The significant perlite reserves in Türkiye are concentrated in Tertiary-Early Middle Quaternary volcanic regions [20]. Perlite reserves in Eastern Anatolia were directly formed by these flows related to young Neogene rhyolitic volcanism and spread over large areas within rhyolite lavas, rhyolitic tuffs, and other volcanic deposits [20]. Nevşehir perlites in Central Anatolia are in the form of secondary domes belonging to the plio-quaternary around the famous Acıgöl crater [20]. Perlites in the Aegean Region are related to the Miocene rhyolitic volcanism of a Mesozoic fold between the Menderes and Karaburun massifs [20]. Within the scope of this study, a total of 126 perlite samples were collected from 12 commercially operated PERQs in Türkiye, given in Fig. 1 and Table S1. Each sample was collected from the upper layers (a depth of 0–5 cm) of each PERQ and placed in polyethylene bag. As reported in previous studies [30–33], the samples were dried, ground and powdered to fit the calibrated powder geometry in the EDXRF spectrometer.

Heavy metal analysis

XRF spectrometry, which performs simultaneous qualitative and quantitative multi-element determinations, is an accurate, fast, sensitive, reliable, simple, and systematic analysis technique [31]. The analysis of HMs (As, Cu, Co, V, Ni, Pb, Zn, Cr, Zr, Mn, Ti and Fe) in the perlite samples was done using EDXRF spectrometer (Spectro Xepos Ametek) with an anode X-ray tube (50 W, 60 kV) having a dual thick Pd/Co mixture. The specifications of the spectrometry and analysis procedure were detailed in previous studies [30–33]. Soil-certified reference material (NIST SRM 2709) was utilized for quality assurance for the EDXRF system. The overall uncertainty of the analytical procedure varied from 0.1% to 16.6%. The detection limit (DL) was calculated given as follows:

$$DL = \frac{3 \times C_i}{N_C} \times \sqrt{\frac{N_B}{t}} \quad (1)$$

where C is the i^{th} elemental concentration, N_B is the background count ratio, N_C is the net count ratio, and t is the counting time [34, 35]. The detection limits of the analyzed

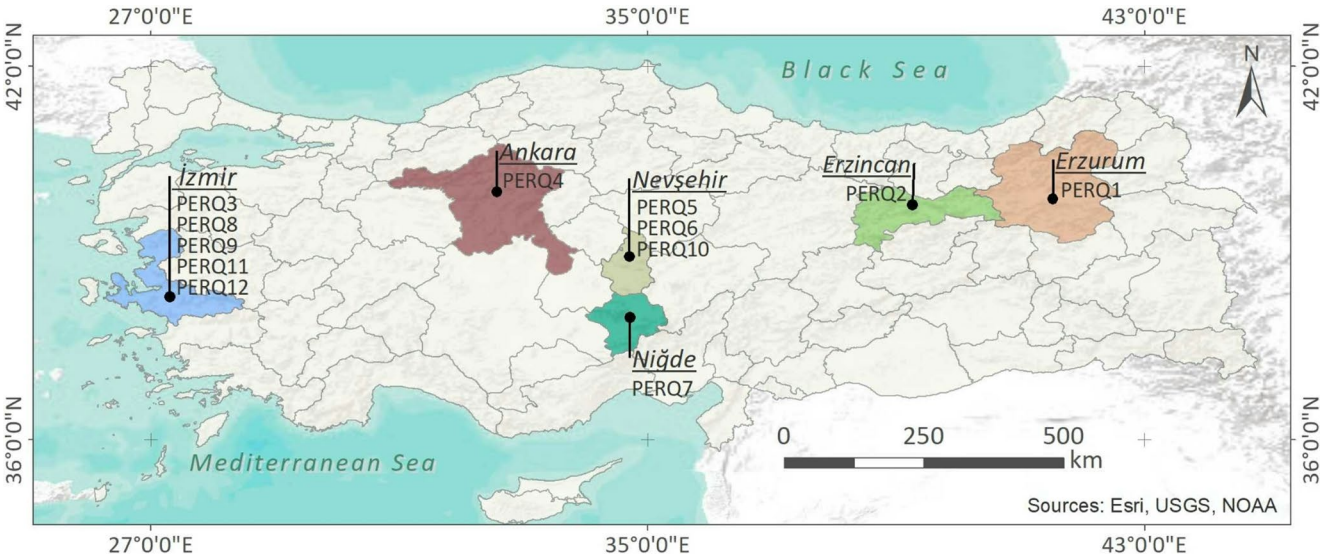

Fig. 1 Locations of perlite quarries in Türkiye

HMs are found as 0.5 (As), 0.5 (Cu), 3.0 (Co), 0.5 (V), 0.6 (Ni), 0.8 (Pb), 0.7 (Zn), 0.3 (Cr), 1.0 (Zr), 1.1 (Mn), 2.0 (Ti), 0.8 (Fe), 2,0 (Cd) and 1.0 (Hg) mg/kg.

Potential health risk assessment

Toxic elements such as HMs in soil, minerals, etc., and environmental samples may pose potential human health risks (PHRs) via three exposure pathways (TEPs): ingestion, inhalation, and dermal contact. In this study, TEPs, including inhalation of particles emitted from perlite, incidental oral ingestion of perlite particles, and dermal contact with perlite, were primarily considered to estimate direct exposure to perlite samples. The average daily intake (ADD in mg/kg· d) in these TEPs within the scope of the PHR evaluation method proposed by the USEPA was calculated for PERQ workers using the following Eqs [32, 36–40]:

$$\mathrm{ADD_{Inh}} = \frac{\mathrm{C} \times \mathrm{InhR} \times \mathrm{EF} \times \mathrm{ED}}{\mathrm{PEF} \times \mathrm{BM} \times \mathrm{AT}} \tag{2}$$

$$\mathrm{ADD_{Ing}} = \frac{\mathrm{C} \times \mathrm{IngR} \times \mathrm{EF} \times \mathrm{ED} \times 10^{-6}}{\mathrm{BM} \times \mathrm{AT}} \tag{3}$$

$$\mathrm{ADD_{Derm}} = \frac{\mathrm{C} \times \mathrm{SA} \times \mathrm{AF} \times \mathrm{ABS} \times \mathrm{EF} \times \mathrm{ED} \times 10^{-6}}{\mathrm{BM} \times \mathrm{AT}} \tag{4}$$

The estimation of the non-carcinogenic PHR refers to the determination of the effect of HMs in perlite samples on non-carcinogenic consequences in PERQ adult workers. Hazard quotient (HQ) and hazard index (HI) are utilized to estimate the non-carcinogenic PHR [32, 39]. HQ was estimated as follows [32, 39]:

$$\mathrm{HQ_{i,Inh}} = \frac{\mathrm{ADD_{i,Inh}}}{\mathrm{R_fD_{i,Inh}}} \tag{5}$$

$$\mathrm{HQ_{i,Ing}} = \frac{\mathrm{ADD_{i,Ing}}}{\mathrm{R_fD_{i,Ing}}} \tag{6}$$

$$\mathrm{HQ_{i,Derm}} = \frac{\mathrm{ADD_{i,Derm}}}{\mathrm{R_fD_{i,Derm}}} \tag{7}$$

$$\mathrm{HQ_i} = \mathrm{HQ_{i,Inh}} + \mathrm{HQ_{i,Ing}} + \mathrm{HQ_{i,Derm}} \tag{8}$$

where $\mathrm{R_fD_{Inh}}$, $\mathrm{R_fD_{Ing,}}$ and $\mathrm{R_fD_{Derm}}$ are the inhalation and ingestion and dermal reference doses, respectively. $\mathrm{HQ_i}$ values estimated for each HM in the perlite sample are summed to obtain the hazard index (HI) as follows [32, 39]:

$$\mathrm{HI} = \sum_{\mathrm{i}=1}^{\mathrm{n}} \mathrm{HQ_i} \tag{9}$$

where n is the number of HMs analyzed in the perlite samples. If HI values are smaller than 1, there is a negligible non-carcinogenic PHR. However, If HI values are higher than 1, the non-carcinogenic PHR may occur with a probability that tends to rise as the increases of HI value [32, 38, 40].

Carcinogenic risk (CR) and total carcinogenic risk (TCR) parameters were estimated using the following formulas to evaluate the carcinogenic effect of HMs on adult workers people [32]:

$$CR_{i,Inh} = ADD_{i,Inh} \times CSF_{i,Inh} \quad (10)$$

$$CR_{i,Ing} = ADD_{i,Ing} \times CSF_{i,Ing} \quad (11)$$

$$CR_{i,Derm} = ADD_{i,Derm} \times CSF_{i,Derm} \quad (12)$$

$$TCR_i = CR_{i,Inh} + CR_{i,Ing} + CR_{i,Derm} \quad (13)$$

where CSF_{Inh}, CSF_{Ing}, and CSF_{Derm} are the inhalation and ingestion and dermal cancer slope factors, respectively. If the TCR values are within the range from $1 \cdot 10^{-6}$ to $1 \cdot 10^{-4}$, there is an acceptable carcinogenic PHR level. If the TCR values are below $1 \cdot 10^{-6}$ there is negligible carcinogenic PHR. However, TCR >1 $\times 10^{-4}$ indicates an unacceptable carcinogenic PHR [32, 38, 40].

All the above parameters and reference values used for the evaluation of PHRs for PERQ adult workers are given in Table S2.

Statistical analysis

Statistical analyses were performed to assess data distribution, examine variance homogeneity, and identify potential differences in HM concentrations among groups. Normality was evaluated using the Shapiro-Wilk test, while the Levene test was applied to assess variance homogeneity. The results indicated that most data did not follow a normal distribution or exhibit homogeneity of variances. To address this, various transformations - including logarithmic, square root, inverse, exponential, Box-Cox, Yeo-Johnson, Z-score, and rank transformation - were applied. Among these, rank transformation yielded the best results. However, even after rank transformation, some data still did not fully meet the assumptions of normality and homogeneity of variances.

For datasets satisfying both normality and variance homogeneity, the ANOVA ($p=0.05$) test was conducted to determine significant differences in HM concentrations, followed by Tukey's post hoc test for pairwise comparisons. In cases where normality and/or variance homogeneity were not achieved, the Kruskal-Wallis test ($p=0.05$) was employed to assess group differences, with pairwise Wilcoxon rank-sum tests used for post hoc analysis.

Additionally, Pearson correlation coefficients were calculated to explore relationships between HM concentrations in perlite samples. All statistical analyses were performed using RStudio version 2023.06 [41].

Spatial distribution

The spatial distribution of HM concentrations in samples was analyzed using QGIS Desktop 3.36.0. For this analysis, the geographic coordinates of each sampling location were mapped onto a digital platform. To estimate HM concentrations across the study area, the inverse distance weighting (IDW) interpolation method was applied, utilizing values obtained from the sampled locations.

Positive matrix factorization (PMF) analysis

In this study, the PMF receptor model was implemented using EPA PMF version 5.0 software [42] to determine the sources of HMs in perlite samples, following the approach outlined by Jiang et al. [43]. The optimal factor solution was identified by evaluating models with 3 to 6 factors, utilizing 20 base runs performed in random seed mode, as described in previous studies [43–45].

Results and discussion

Heavy metal content

Some descriptive statistical data on the concentrations of HMs analyzed in all perlite samples and the contents of Earth's upper crust (EUC) are given in Table 1. The frequency distributions of each HM after rank transformation are shown in Fig. 2. Following the transformation, all HMs, except V and Co, exhibit a normal distribution ($p<0.05$). Although V and Co deviate from normality, the rank transformation still provides the best distribution compared to other applied transformations. The average and range (min-max) values of HMs analyzed in PERQs are given in Table S3. The spatial distribution of HMs is presented in Fig. 3, illustrating how they exhibit distinct distribution patterns across different locations. From Table 1 and S3, the concentrations of the HMs in perlite samples vary depending on the geological and geochemical structure of the PERQ locations. The average concentrations of the HMs were ranked as As <Cu<Co<V<Ni<Pb<Zn<Cr<Zr<Mn<Ti<Fe. The concentrations of Cd and Hg were analyzed below the DL of 2.0 and 1.0 mg/kg, respectively.

From Table 1, the As concentrations varied from < 0.5 to 9.0 (PERQ12-5) mg/kg with an average value of 4.2 mg/kg, which is lower than the EUC value of 4.8 mg/kg [46]. From Table S3, the As contents of the quarries coded PERQ3, PERQ5 (except for PERQ5-3), PERQ9, and PERQ12 are above the EUC value. According to the average As contents, the quarries were listed as PERQ3 >PERQ12 >PERQ9 >PERQ5 >PERQ7 >PERQ10 >PERQ8 >PERQ11 >PERQ4 >PERQ6 >PERQ2 >PERQ1. The Cu concentrations varied from 1.1 to 19.7 (PERQ4-2) mg/kg with an average value of 4.3 mg/kg, which is significantly lower than the EUC value of 28 mg/kg [46]. According to the average Cu contents, the quarries were listed as PERQ4 >PERQ8 >PERQ5 >PERQ1 >PERQ6 >PERQ10 >PERQ11 >PERQ2 >PERQ12 >PERQ3 >PERQ9 >PERQ7. The cobalt

Table 1 Some descriptive statistical data on concentrations of heavy metals in all perlite samples

HM	Concentration (mg/kg, dw)								EUC (mg/kg)
	Average	Median	SD	SE	Kurtosis	Skewness	Min	Max	
Ti	528.3	515.4	214.3	19.1	0.1	0.7	117.1	1361.0	3931
V	7.1	6.9	3.5	0.3	0.4	−0.8	< DL	14.7	97
Cr	64.9	50.1	57.6	5.1	1.2	1.2	< DL	247.1	92
Mn	383.5	378.8	73.5	6.5	0.4	−0.2	257.3	640.9	774.5
Fe	6585.4	6255.5	1626.3	144.9	0.6	0.2	3914.0	12730.0	32041
Co	7.0	6.4	1.8	0.2	2.4	5.9	< DL	13.9	17.3
Ni	19.8	16.4	15.7	1.4	1.8	3.4	4.6	77.7	47
Cu	4.3	3.4	3.4	0.3	2.5	6.7	1.1	19.7	28
Zn	31.1	31.8	6.4	0.6	−0.4	−0.8	17.0	45.7	67
As	4.2	3.5	2.3	0.2	0.4	−1.3	< DL	9.0	4.8
Pb	26.4	24.4	7.2	0.6	0.4	−1.1	15.1	41.6	17
Zr	93.7	88.0	28.3	2.5	0.2	−0.9	40.5	163.1	193

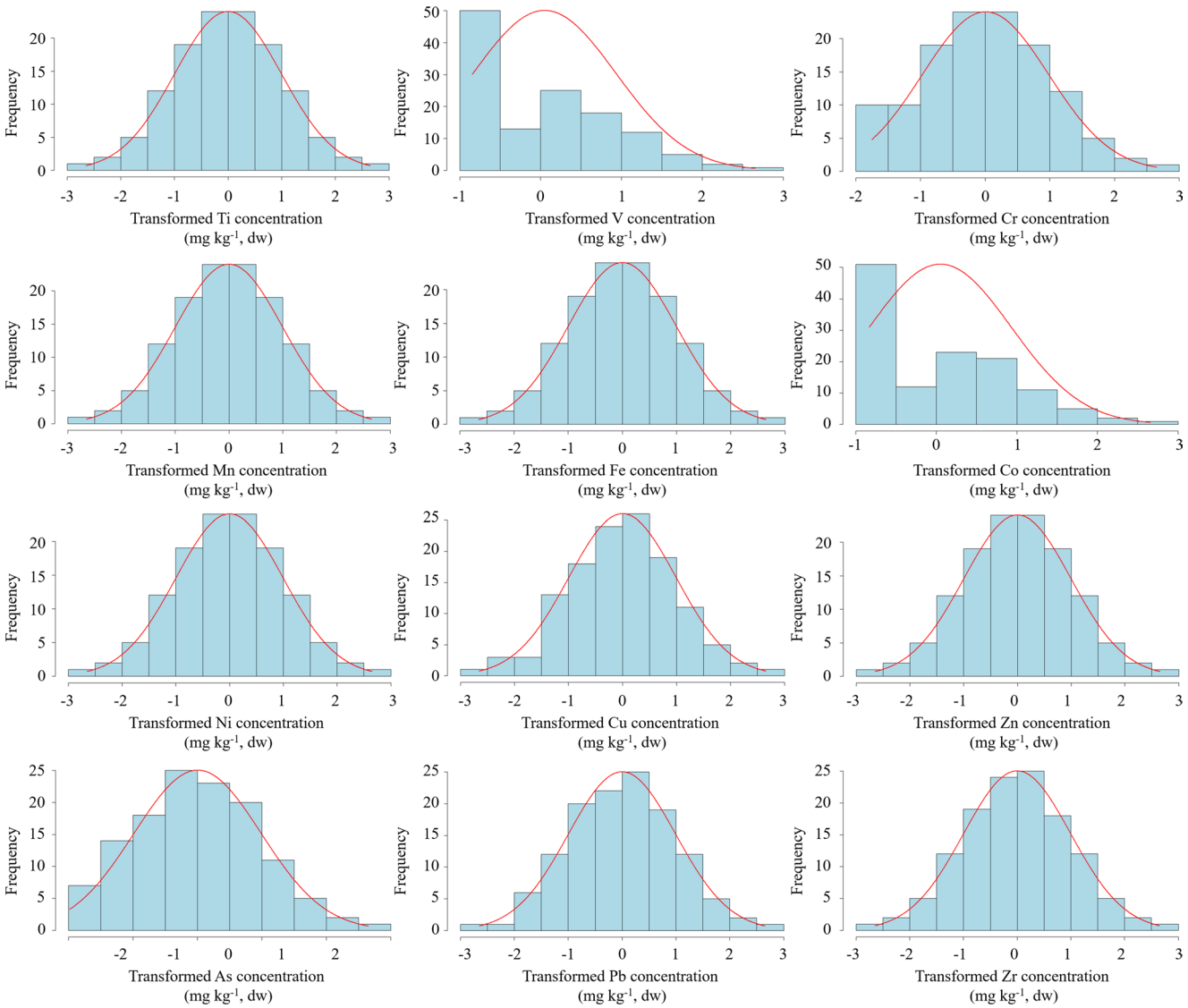

Fig. 2 The frequency distribution of HMs after rank transformation

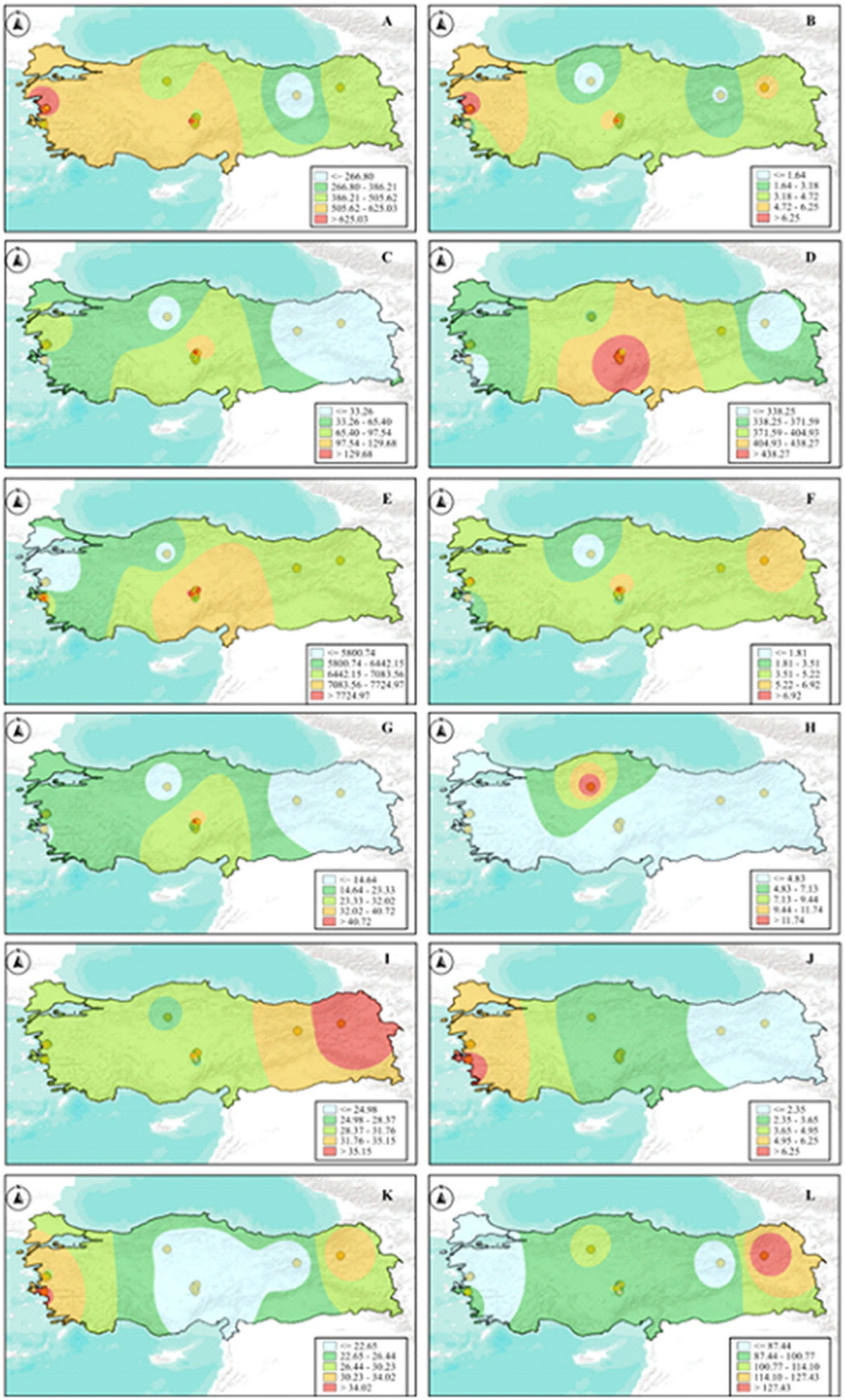
A
<= 266.80
266.80 - 386.21
386.21 - 505.62
505.62 - 625.03
> 625.03
B
<= 1.64
1.64 - 3.18
3.18 - 4.72
4.72 - 6.25
> 6.25
C
<= 33.26
33.26 - 65.40
65.40 - 97.54
97.54 - 129.68
> 129.68
D
<= 338.25
338.25 - 371.59
371.59 - 404.93
404.93 - 438.27
> 438.27
E
<= 5800.74
5800.74 - 6442.15
6442.15 - 7083.56
7083.56 - 7724.97
> 7724.97
F
<= 1.81
1.81 - 3.51
3.51 - 5.22
5.22 - 6.92
> 6.92
G
<= 14.64
14.64 - 23.33
23.33 - 32.02
32.02 - 40.72
> 40.72
H
<= 4.83
4.83 - 7.13
7.13 - 9.44
9.44 - 11.74
> 11.74
I
<= 24.98
24.98 - 28.37
28.37 - 31.76
31.76 - 35.15
> 35.15
J
<= 2.35
2.35 - 3.65
3.65 - 4.95
4.95 - 6.25
> 6.25
K
<= 22.65
22.65 - 26.44
26.44 - 30.23
30.23 - 34.02
> 34.02
L
<= 87.44
87.44 - 100.77
100.77 - 114.10
114.10 - 127.43
> 127.43

Fig. 3 The spatial distribution of HMs (mg/kg) (**a**) Ti, (**b**) V, (**c**) Cr, (**d**) Mn, (**e**) Fe, (**f**) Co, (**g**) Ni, (**h**) Cu, (**i**) Zn, (**j**) As, k) Pb, l) Zr

(Co) concentrations varied from < DL to 13.9 (PERQ5-2) mg/kg with an average value of 7.0 mg/kg, which is lower than the EUC value of 17.3 mg/kg [46]. The Co contents of the quarries coded PERQ3, PERQ4, and PERQ7 were observed below the DL of 3.0 mg/kg. According to the average Co contents, the quarries were listed as PERQ5 >PERQ8 >PERQ6 >PERQ10 >PERQ1 >PERQ9 >PERQ12 >PERQ11 >PERQ2. The vanadium (V) concentrations varied from < DL to 14.7 (PERQ9-15) mg/kg with an average value of 7.1 mg/kg, which is significantly lower than the EUC value of 97 mg/kg [46]. The V contents of the quarries coded PERQ3, PERQ4, and PERQ7 were observed below the DL of 0.5 mg/kg. According to the average V contents, the quarries were listed as PERQ1 >PERQ11 >PERQ12 >PERQ9 >PERQ10 >PERQ5 >PERQ2 < PERQ6 < PERQ8. The Ni concentrations varied from 4.6 to 77.7 (PERQ5-5) mg/kg with an average value of 19.8 mg/kg, which is lower than the EUC value of 47 mg/kg [46]. However, the Ni contents of the quarries coded PERQ5 are above the EUC value. According to the average Ni contents, the quarries were listed as PERQ5 >PERQ8 >PERQ6 >PERQ7 >PERQ12 >PERQ10 >PERQ9 >PERQ11 >PERQ3 >PERQ2 >PERQ1 >PERQ4. The Pb concentrations varied from 15.1 to 41.6 (PERQ3-7) mg/kg with an average value of 26.4 mg/kg. All Pb concentrations, except for three perlite samples, are higher than the EUC value of 17 mg/kg [46]. According to the average Pb contents, the quarries were listed as PERQ3 >PERQ1 >PERQ12 >PERQ9 >PERQ11 >PERQ10 >PERQ4 >PERQ6 >PERQ2 >PERQ8 >PERQ5 >PERQ7. The Zn concentrations varied from 17.0 to 45.7 (PERQ10-10) mg/kg with an average value of 31.1 mg/kg, which is lower than the EUC value of 67 mg/kg [46]. According to the average Zn contents, the quarries were listed as PERQ1 >PERQ12 >PERQ6 >PERQ10 >PERQ11 >PERQ2 >PERQ3 >PERQ9 >PERQ4 >PERQ8 >PERQ4 >PERQ7. The Cr concentrations varied from < 0.3 to 247.1 (PERQ5-1) mg/kg with an average value of 64.9 mg/kg, which is lower than the EUC value of 92 mg/kg [46]. However, the Cr contents of the quarries coded PERQ5, PERQ6, and PERQ8 are above the EUC value. According to the average Cr contents, the quarries were listed as PERQ5 >PERQ8 >PERQ6 >PERQ7 >PERQ12 >PERQ10 >PERQ11 >PERQ9 >PERQ3 >PERQ2 >PERQ1 >PERQ4. The zirconium (Zr) concentrations varied from 40.5 to 163.1 (PERQ10-10) mg/kg with an average value of 93.7 mg/kg, which is lower than the EUC value of 193 mg/kg [46]. According to the average Zr contents, the quarries were listed as PERQ1 >PERQ6 >PERQ10 >PERQ11 >PERQ4 >PERQ3 >PERQ8 >PERQ12 >PERQ2 >PERQ7 >PERQ9 >PERQ5. The Mn concentrations varied from 257.3 to 640.9 (PERQ10-10) mg/kg with an average value of 383.5 mg/kg, which is lower than the EUC value of 774.5 mg/kg [46]. According to the average Mn contents, the quarries were listed as PERQ10 >PERQ11 >PERQ5 >PERQ7 >PERQ6 >PERQ8 >PERQ2 >PERQ4 >PERQ12 >PERQ1 >PERQ3 >PERQ9. The titanium (Ti) concentrations varied from 117.1 to 1361.0 (PERQ10-10) mg/kg with an average value of 528.3 mg/kg, which is lower than the EUC value of 3931 mg/kg [46]. According to the average Ti contents, the quarries were listed as PERQ10 >PERQ11 >PERQ12 >PERQ9 >PERQ6 >PERQ3 >PERQ1 >PERQ8 >PERQ4 >PERQ7 >PERQ5 >PERQ2. The Fe concentrations varied from 3914.0 to 12730.0 (PERQ10-10) mg/kg with an average value of 6583.4 mg/kg, which is lower than the EUC

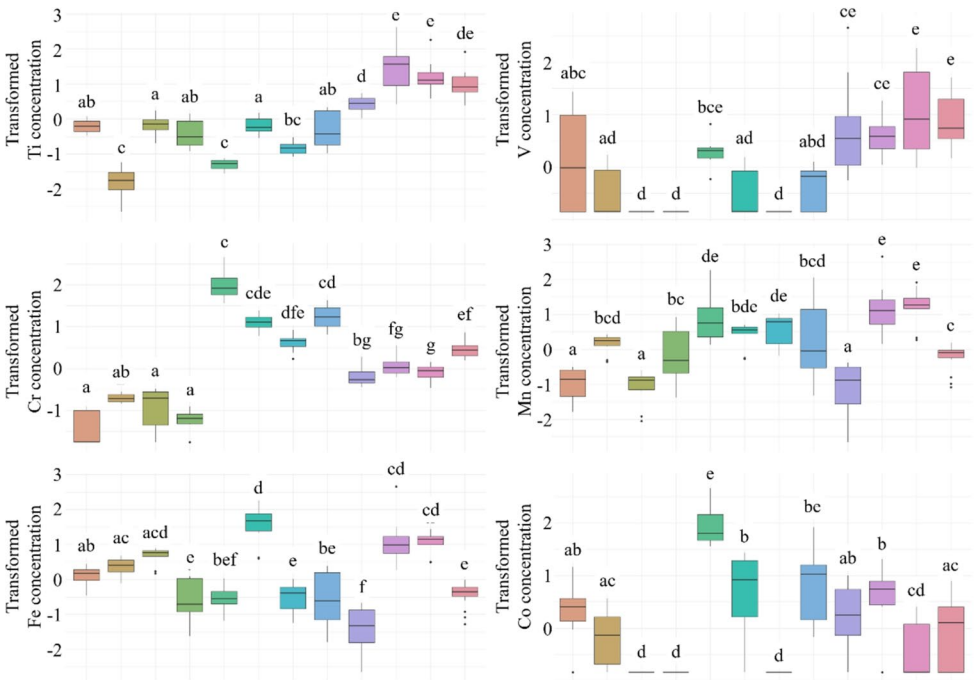

Fig. 4 Distribution of transformed concentrations for heavy metals across sampling locations. Letters above each boxplot denote statistically significant differences ($p < 0.05$) between locations, with shared letters indicating no significant difference

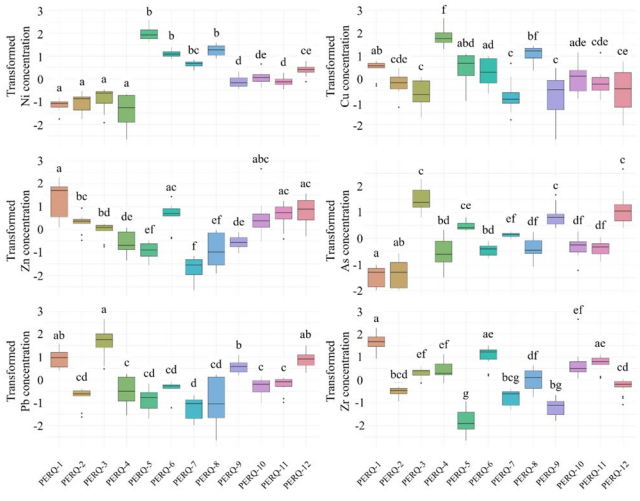

Fig. 4 (continued)

value of 32,041 mg/kg [46]. According to the average Fe contents, the quarries were listed as PERQ6 >PERQ10 >PERQ11 >PERQ3 >PERQ2 >PERQ1 >PERQ12 >PERQ8 >PERQ7 >PERQ5 >PERQ4 >PERQ9.

Variability of HMs in sampling locations

The distribution of HMs among different locations is presented in Fig. 4. Box plots of transformed elemental concentrations reveal significant spatial variability across the sampling locations (PERQ-1 to PERQ-12). For example, Ti and V concentrations exhibit a marked increase in the latter PERQ locations (PERQ-8 to PERQ-12), while Cr concentrations peak significantly at PERQ-5 compared to earlier sites. Fe concentrations display a notable peak at PERQ-6, and Co shows a similar trend at PERQ-5. Mn concentrations vary spatially, with PERQ-5 showing significantly higher levels than PERQ-1, PERQ-2, PERQ-3, and PERQ-4, though generally decreasing toward the later PERQ locations. Similarly, Ni concentrations are low across PERQ-1 to PERQ-4 but increase significantly at PERQ-5. Cu exhibits peak concentrations at PERQ-4 and PERQ-8, while Zn is markedly elevated at PERQ-1, decreases toward PERQ-6, and then rises again in subsequent locations. As concentrations are highest at PERQ-3 and again after PERQ-9. Pb concentrations are significantly higher at PERQ-1 and PERQ-3, with lower levels observed at PERQ-2, across PERQ-4 to PERQ-8, and at PERQ-10 and PERQ-11, whereas Zr shows elevated levels at PERQ-1, a substantial decrease at PERQ-5, and then an increase toward PERQ-12.

Statistical analysis - indicated by letter groupings above each box plot - reveals significant differences ($p<0.05$) in transformed concentrations between certain sampling locations for each element. This emphasizes both the localized impact of geochemical processes and the overall spatial heterogeneity of elemental distribution within the study area.

Overall, the elemental distribution patterns suggest distinct geochemical regimes across the sampling area. Some locations - for instance, PERQ-1, PERQ-3, PERQ-5, PERQ-6, and PERQ-8 (or the broader group from PERQ-8 to PERQ-12 for certain elements) - exhibit enhanced HM concentrations, possibly indicative of localized source inputs or accumulation processes. In contrast, other areas, such as PERQ-2 and zones spanning PERQ-4 to PERQ-7 and PERQ-10 to PERQ-11, tend to have relatively lower concentrations. These unique elemental signatures underscore the heterogeneity of the study area and highlight the localized impacts of both geochemical and potentially anthropogenic factors on HM distribution.

PMF analysis results

To identify potential sources of HMs in perlite samples, Pearson correlation analysis was conducted to examine pairwise relationships among HMs, while the PMF model was applied to determine possible common sources contributing to their presence [43]. The analysis identified three distinct factors as sources of HMs. According to the PMF model results, Factor 1 accounted for 75.10% of the total contribution, followed by Factor 3 at 19.20% and Factor 2 at 5.70% (Fig. 5a). Figure 5b presents the contribution of each HM to the factors identified in the PMF model. Based on the PMF analysis (Fig. 5c), the HM sources in the study area can be classified into three factors with distinct elemental signatures. Factor 1 is dominated by Ti (75.1%), V (76.66%), As (62.52%), and Pb (65.82%), with substantial contributions from Co (53.89%) and Zn (51.97%). Potential sources of Ti include geogenic origins, mining activities, and mining waste [47]. Similarly, As is primarily associated with natural sources [48, 49], whereas Pb [50], Co [51], and Zn [52] have been linked to anthropogenic activities. Given this combination, it is plausible that Factor 1 primarily represents the influence of natural soil, with additional contributions from anthropogenic sources.

Factor 2 is characterized by very high contributions of Cr (89.32%) and Ni (69.13%). Previous studies have shown that Cr in the environment is closely associated with industrial activities, including leather processing, refractory steel production, and the manufacture of chromic acids [53, 54]. This evidence supports the interpretation of Factor 2 as being predominantly industrial in origin.

Factor 3 exhibits elevated contributions from Fe (55.26%), Mn (44.05%), Cu (44.12%), Zn (42.47%), and Zr (53.35%), with moderate inputs from Pb (33.39%) and Ni (21.85%). Among these metals, Fe, Mn, and Zr are predominantly of natural origin [47]. In contrast, Cu and Zn may be linked to agricultural sources, including fertilization, pesticides, livestock manure, and wastewater, as these elements

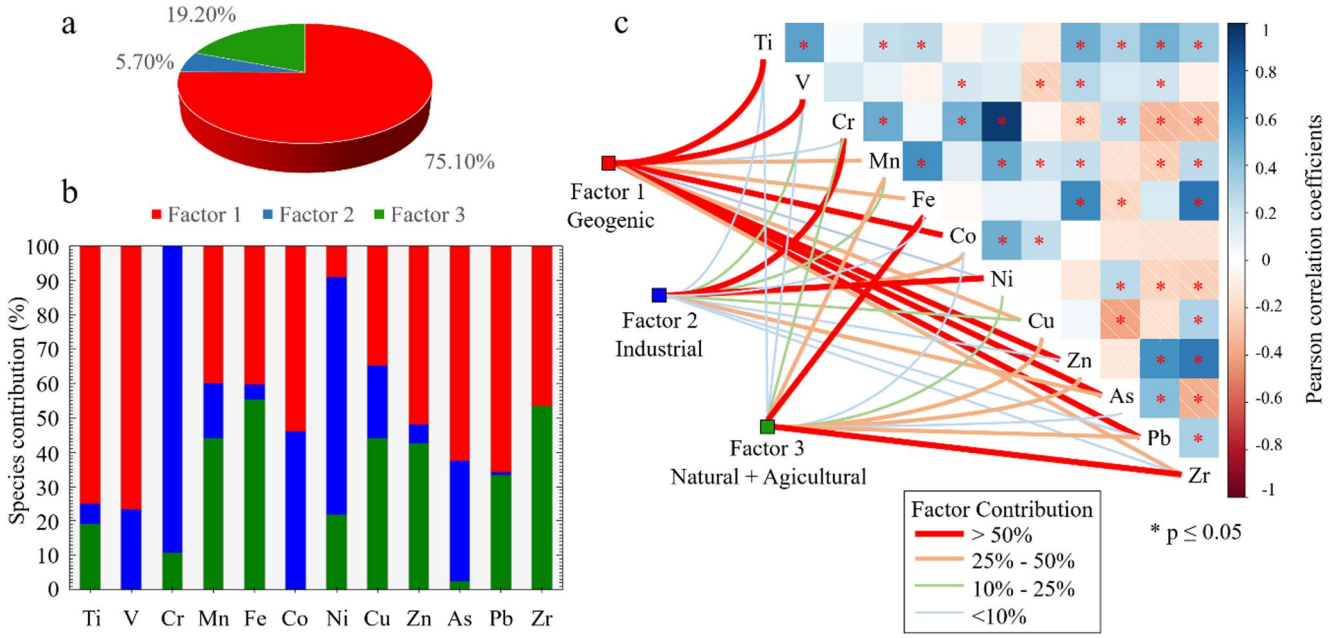

Fig. 5 Pearson correlation and PMF model results

are commonly enriched in agricultural soils [11, 55]. Therefore, Factor 3 appears to represent a mixed source, combining natural inputs with agricultural influences.

Assessment of potential health risk

The values of ADD_i, HQ_i, HI, CR_i, and TCR estimated for PERQ workers to evaluate the non-carcinogenic and carcinogenic PHRs due to each HM analyzed in perlite samples are given in Table 2 [56].The average values of the ADD_{Inh}, ADD_{Ing} and ADD_{Derm} calculated for all HMs varied from 8.1×10^{-11} to 1.4×10^{-6} mg/kg· d, 5.5×10^{-7} to 9.4×10^{-3} mg/kg· d, and 3.5×10^{-9} to 6.2×10^{-5} mg/kg· d, respectively. The trends of the average of total ADD for HMs in all perlite were As < Ni < Pb < Cu < Cr < Co < V < Zn < Zr < Mn < Ti < Fe.

The average values of the HQ_{Inh}, HQ_{Ing}, and HQ_{Derm} estimated for all HMs in the perlite samples were 5.8×10^{-3}, 2.5×10^{-2} and 5.0×10^{-3}, respectively. The averages of the total HQ estimated for three TEPs were listed as Fe > Mn > Cr > As > V > Pb > Co > Ni > Cu > Zn. Concerning average HQ_i, the three TEPs were ingestion > inhalation > dermal contact. The HI value was estimated as 0.036, which is below the risk limit of 1.

The average values of the CR_{Ing}, CR_{Inh}, and CR_{Derm} estimated for Pb, Cr, As and Ni were found to be 5.4×10^{-8}, 9.1×10^{-6} and 1.5×10^{-5}, respectively. The averages of the

Table 2 Impact of heavy metals in perlite samples by three exposure routes on quarry adult workers

HM	Non-carcinogenic risk						Carcinogenic risk			
	ADD (mg/kg· d)			HQ_i			CR_i			
	Inhalation	Ingestion	Dermal	Inhalation	Ingestion	Dermal		Inhalation	Ingestion	Dermal
Ti	1.1×10^{-7}	7.5×10^{-4}	5.0×10^{-6}	-	-	-		-	-	-
Zr	2.0×10^{-8}	1.3×10^{-4}	8.8×10^{-7}	-	-	-		-	-	-
V	1.5×10^{-9}	1.0×10^{-5}	6.7×10^{-8}	2.1×10^{-7}	1.1×10^{-3}	9.6×10^{-4}		-	-	-
Cu	9.1×10^{-10}	6.2×10^{-6}	4.1×10^{-8}	2.3×10^{-8}	1.5×10^{-4}	3.4×10^{-6}			-	-
Mn	$8.1E\times10^{-8}$	5.5×10^{-4}	3.6×10^{-6}	5.8×10^{-3}	3.9×10^{-3}	2.0×10^{-3}		-	-	-
Fe	$1.4E\times10^{-6}$	9.4×10^{-3}	6.2×10^{-5}	2.0×10^{-6}	1.3×10^{-2}	8.9×10^{-4}		-	-	-
Co	$1.5E\times10^{-9}$	1.0×10^{-5}	6.1×10^{-8}	6.5×10^{-8}	4.9×10^{-4}	4.1×10^{-6}		-	-	-
Zn	$6.5E\times10^{-8}$	4.4×10^{-5}	2.9×10^{-7}	2.2×10^{-8}	1.5×10^{-4}	4.9×10^{-6}		-	-	-
Cr	$1.2E\times10^{-9}$	8.6×10^{-6}	5.6×10^{-7}	4.4×10^{-5}	2.8×10^{-3}	1.9×10^{-4}		5.3×10^{-8}	4.3×10^{-6}	$1.\times10^{-5}$
Ni	$3.8E\times10^{-10}$	2.6×10^{-6}	1.7×10^{-7}	1.8×10^{-8}	1.3×10^{-4}	2.2×10^{-4}		3.2×10^{-10}	4.4×10^{-6}	3.9×10^{-6}
As	$8.1E\times10^{-11}$	5.5×10^{-7}	3.5×10^{-8}	2.7×10^{-7}	1.8×10^{-3}	3.0×10^{-4}		1.2×10^{-9}	7.9×10^{-7}	1.3×10^{-7}
Pb	$5.1E\times10^{-10}$	3.5×10^{-6}	2.3×10^{-7}	1.5×10^{-7}	9.9×10^{-4}	4.4×10^{-4}		2.1×10^{-11}	3.0×10^{-8}	6.5×10^{-9}
				$HI_i=\Sigma HQ_i$	$5.8E\times10^{-3}$	2.5×10^{-2}	5.0×10^{-3}	$TCR_i=\Sigma CR_i$	5.4×10^{-8}	9.5×10^{-6}	1.5×10^{-5}
				$HI=\Sigma HI_i$	3.6×10^{-2}			$TCR=\Sigma TCR_i$	2.5×10^{-5}		

total CR_i estimated for three TEPs were listed as Cr>Ni>As >Pb. Concerning average CR_i, the three TEPs were ordered as dermal>ingestion>inhalation. The TCR value estimated for these four HMs and three exposure routes is 2.5×10^{-5}, which is below the carcinogenic risk limit of 1.0×10^{-4}. Figure 6 displays radarcharts illustrating the spatial variability of the HI

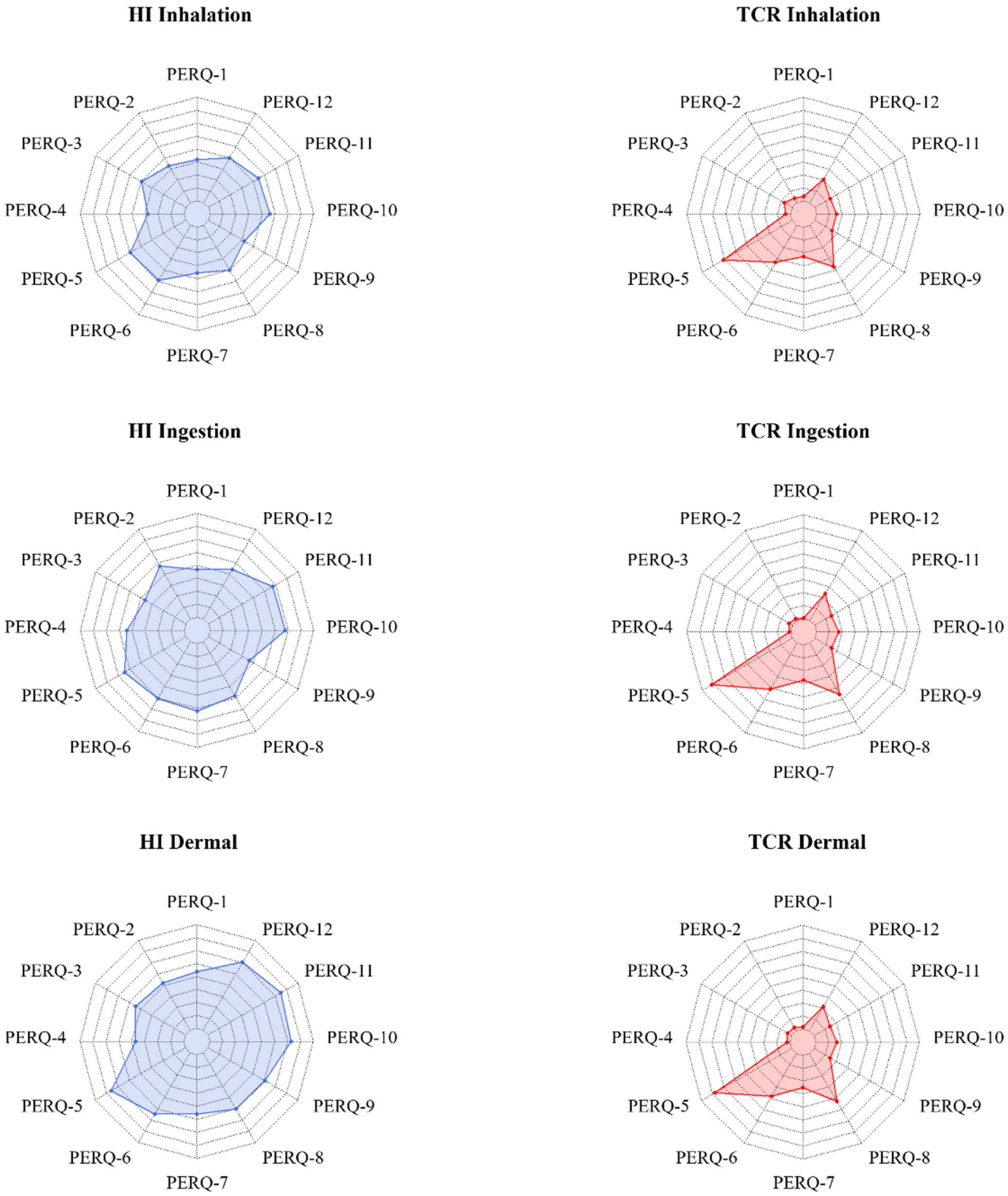

Fig. 6 The radarchart of HI and TCR values for sampling locations

and TCR across sampling locations (PERQ-1 to PERQ-12) via three exposure pathways: inhalation, ingestion, and dermal contact. Blue-shaded areas represent HI values, indicating the potential for non-carcinogenic health effects, while red-shaded areas represent TCR values, reflecting the excess lifetime cancer risk. Variations in the shape and size of the shaded areas across locations and exposure routes highlight the heterogeneity of potential health risks within the study area. Locations with larger shaded areas indicate a greater potential for both non-carcinogenic and carcinogenic adverse health effects.

Conclusion

In this study, for the first time, the distributions of 26 HMs in perlite samples from commercially operated 12 PERQs in Türkiye were determined by the EDXRF spectrometry. Also, for the first time, based on the HM contents analyzed in perlite samples, carcinogenic and non-carcinogenic potential health risks for adult quarry workers were assessed. All Pb concentrations, except for three perlite samples, are higher than those in Earth's upper crust. Potential health risk assessment is a critical approach used to estimate the significant risks that arise when workers in perlite quarries or end users of perlite as an additive material come into contact with toxic heavy metal contaminants. The results revealed that HQ, HI, CRI, and TRC values are all within safe levels.

Consequently, the data obtained is information that can create awareness for both perlite quarry workers and consumers. In addition, the distribution of toxic HMs in the quarries can form a prospective database. Even if the estimated risk parameters are within safety limits, situations that could threaten the health of employees may arise. In such cases, the Ministry of Labor and Social Security of the Republic of Turkey should inspect such mines, and necessary precautions, such as preventing employees from breathing perlite dust, should be mandatory and controlled.

Supplementary Information The online version contains supplementary material available at https://doi.org/10.1007/s12665-025-12654-x.

Acknowledgements This study is carried out within the framework of a doctoral thesis performed at Kastamonu University and The Scientific Research Projects Coordinator of Kastamonu University (Research Projects codded of KÜBAP-01/2022-04 and KÜ-HIZDES/2023/2/40).

Author contributions Şeref Turhan; Conceptualization, Data curation, Formal analysis, Methodology, Writing - original draft, Writing - review editing. Savaş Türkdoğan: Visualization, Methodology, Resources. Ergin Murat Altuner: Formal analysis, Methodology, Writing - review editing. Aslı Kurnaz: Visualization, Methodology, Resources. Aybaba Hançerlioğulları: Investigation, Resources.

Data availability Not applicable.

Declarations

Competing interests The authors declare no competing interests.

References

1. Tchounwou PB, Yedjou CG, Patlolla AK, Sutton DJ (2012) Heavy metal toxicity and the environment. Exp Suppl 101:133–164
2. Ali H, Khan E, Ilahi I (2019) Environmental chemistry and ecotoxicology of hazardous heavy metals: environmental persistence, toxicity, and bioaccumulation. J Chem 2019:1–15
3. Briffa J, Sinagra E, Blundell R (2020) Heavy metal pollution in the environment and their toxicological effects on humans. Heliyon 6(9):1–26
4. Karn R, Ojha N, Abbas S, Bhugra S (2021) A review on heavy metal contamination at mining sites and remedial techniques. IOP Conf Ser: Earth Environ Sci 796:1–30
5. Das S, Sultana KW, Ndhlala AR, Mondal M, Chandra I (2023) Heavy metal pollution in the environment and its impact on health: exploring green technology for remediation. Environ Health Insights 17:1–10
6. Hadzi G (2022) In: Saleh HM, Amal I, Hassan (eds) Effect of mining on heavy metals toxicity and health risk in selected rivers of Ghana, chapters. Environmental Impact and Remediation of Heavy Metals, IntechOpen
7. Eziz M, Mohammad A, Mamut A, Hini G (2018) A human health risk assessment of heavy metals in agricultural soils of Yanqi Basin, silk road economic Belt, China. Hum Ecol Risk Assess 24(5):1352–1366
8. Sall ML, Diaw AKD, Gningue-Sall D, Aaron AE, Aaron JJ (2020) Toxic heavy metals: impact on the environment and human health, and treatment with conducting organic polymers, a review. Environ Sci Pollut Res Int 27(24):29927–29942
9. Fodoué Y, Ismaila A, Yannah M, Wirmvem MJ, Mana CB (2022) Heavy metal contamination and ecological risk assessment in soils of the Pawara gold mining Area, Eastern Cameroon. Earth 3:907–924
10. Haghighizadeh A, Rajabi O, Nezarat A, Hajyani Z, Haghmohammadi M, Hedayatikhah S, Asl SD, Beni AA (2024) Comprehensive analysis of heavy metal soil contamination in mining environments: Impacts, monitoring Techniques, and remediation strategies. Arab J Chem 17(6):1–26
11. Li Z, Ma Z, van der Kuijp TJ, Yuan Z, Huang L (2014) A review of soil heavy metal pollution from mines in china: pollution and health risk assessment. Sci Total Environ 468(469):843–853
12. Fashola MO, Ngole-Jeme VM, Babalola OO (2016) Heavy metal pollution from gold mines: environmental effects and bacterial strategies for resistance. Int J Environ Res Public Health 13(11):1–20
13. Qi Y, Wei X, Zhao M, Pan W, Jiang C, Wu J, Li W (2022) Heavy metal pollution characteristics and potential ecological risk assessment of soils around three typical antimony mining areas and watersheds in China. Front Environ Sci 10:1–13
14. Adnan M, Xiao B, Ali MU, Xiao P, Zhao P, Wang H, Bibi S (2024) Heavy metals pollution from smelting activities: a threat to soil and groundwater. Ecotoxicol Environ Saf 274:1–12
15. Hao W, Liu H, Hao S, Mao K (2024) Characterization of heavy metal contamination in groundwater of typical mining area in Hunan Province. Sci Rep 14:1–12
16. Vijayaraghavan K, Raja FD (2014) Experimental characterisation and evaluation of perlite as a sorbent for heavy metal ions in single and quaternary solutions. J Water Process Eng 4:179–184

17. Maxim LD, Niebo R, McConnell EE (2014) Perlite toxicology and epidemiology-a review. Inhal Toxicol 26(5):259–270
18. Khoshraftar Z, Masoumi H, Ghaemi A (2023) On the performance of perlite as a mineral adsorbent for heavy metals ions and dye removal from industrial wastewater: A review of the state of the Art. Case Stud Chem Environ Eng 8:1–17
19. Angelopoulos PM (2024) Insights in the physicochemical and mechanical properties and characterization methodology of perlites. Minerals 14(1):1–25
20. DPT (Devlet Planlama Teşkilatı) (2001) Madencilik Özel İhtisas Komisyonu Raporu. Endüstriyel Hammaddeler Alt Komisyonu Yapı Malzemeleri III (Pomza-Perlit-Vermikülit-Flogopit-Genleşen Killer) Çalışma Grubu Raporu. DPT: 2617- ÖİK: 628, Ankara (in Turkish)
21. Najafi P, Asgari K, Samadi N (2016) Heavy metal elimination from industrial wastewater using natural substrate on pitcher irrigation. Int J Recycl Org Waste Agricult 5:333–337
22. Ates A, Altintig E, Demirel H, Yilmaz M (2017) Comparative study on adsorptive removal of Cu, Pb, Zn heavy metals by modified perlite composites. Desalin Water Treat 98:244–253
23. Petrella A, Spasiano D, Rizzi V, Cosma P, Race M, De Vietro N (2018) Lead ion sorption by perlite and reuse of the exhausted material in the construction field. Appl Sci 8(10):1–13
24. Turp MS (2019) Adsorption kinetics and isotherms of Ni (II) and Zn (II) heavy metals onto a natural adsorbent: expanded perlite. Desalin Water Treat 142:205–212
25. Wang J, Zhu Y, Jiang Z, Du X, Zheng M, Li L, Ni H, Wang Y, Li Z, Li Q (2024) Characteristics and mechanism of Ni2 + and Cd2 + adsorption by recovered perlite from agar extraction residue. Chin J Chem Eng 72:141–152
26. Karua PÇ, Arifuzzaman Md, Islam MS (2024) Effects of perlite content and jute fiber reinforcement on flexural behavior of the gypsum/perlite composite core-based sandwich structures. Constr Build Mater 441:1–11
27. Tsardaka EC, Tsampali E, Stefanidou M (2024) Assessment of perlite by-product as pozzolanic material in cement pastes. J Build Eng 91:1–19
28. Fang C, Wen J, Li Y, Liu L, Shi Y, Lyu Y, Xing B, Yang J (2025) Effects of the modified expanded perlite materials on magnesium phosphate cement-based fireproof mortars: mechanical property, thermal conductivity and microstructure. Case Stud Constr Mater 22:1–11
29. Kandilli C, Gür M, Yilmaz H, Öztop HF (2025) Experimental and numerical analyses of a model trombe wall employing the natural zeolite/perlite composite plate as a thermal mass for nearly zero energy buildings. Int Commun Heat Mass Transf 160:1–13
30. Turhan Ş, Tokat S, Kurnaz A, Altıkulaç A (2022) Distribution of elemental compositions of zeolite quarries and calculation of radiogenic heat generation. Int J Environ Anal Chem 109(19):7851–7862
31. Altıkulaç A, Turhan Ş (2023) Assessment of the levels of potentially toxic elements contained in natural bentonites collected from quarries in Turkey. ACS Omega 8(23):20797–20986
32. Turhan Ş, Altuner EM, Bakır TK, Duran C, Hançerlioğulları A, Kurnaz A (2025) Assessment of human health risk caused by heavy metals in kiln dust from coal-fired clay brick factories in Türkiye. Expo Health 30:303–312
33. Turhan Ş, Altuner EM, Ayata A, Gezer F, Hançerlioğulları A, Kurnaz A, Karataşlı M (2025) Dispersion of oxides, heavy metals, and natural radionuclides in phosphogypsum stockpiles of the phosphate industries in Türkiye. Environ Sci Pollut Res 32:7692–7704
34. Van Grieken R, Markowicz A (2001) Handbook of X-Ray spectrometry. CRC
35. Baltas H, Sirin M, Gökbayrak E, Ozcelik AE (2020) A case study on pollution and a human health risk assessment of heavy metals in agricultural soils around Sinop Province. Turk Chemosphere 241:1–10
36. USEPA (United States Environmental Protection Agency) (1989) Risk assessment guidance for superfund. Volume I: Human health evaluation manual (Part A), EPA/540/1–89/002, Washington, DC
37. USEPA (United States Environmental Protection Agency), (2004) Risk assessment guidance for superfund. Volume 1: Human Health Evaluation Manual (Part E, Supplemental Guidance for Dermal Risk Assessment). EPA/540/R/99/005, Office of Superfund Remediation and Technology Innovation, U.S. Environmental Protection Agency Washington, DC
38. USEPA (United States Environmental Protection Agency) (2011) Exposure factors handbook (Final Report). Chapter 5: soil and dust ingestion. U.S. Environmental Protection Agency, Washington, DC
39. Miletić A, Lučić M, Onjia A (2023) Exposure factors in health risk assessment of heavy metal(loid)s in soil and sediment. Metals 13(7):1–28
40. Ma J, Chen L, Chen H, Wu D, Ye Z, Zhang H, Liu D (2023) Spatial distribution, sources, and risk assessment of potentially toxic elements in cultivated soils using isotopic tracing techniques and Monte Carlo simulation. Ecotoxicol Environ Saf 259:1–12
41. Team RC (2025) A language and environment for statistical computing. R Foundation for Statistical Computing, Vienna, Austria. https://www.R-project.org/. Accessed 2025
42. USEPA (United States Environmental Protection Agency) (2014) EPA positive matrix factorization (PMF) 5.0 fundamentals and user guide. U.S. Environment Protection Agency, Washington, DC
43. Jiang W, Meng L, Liu F, Sheng Y, Chen S, Yang J, Mao H, Zhang J, Zhang Z, Ning N (2023) Distribution, source investigation, and risk assessment of topsoil heavy metals in areas with intensive anthropogenic activities using the positive matrix factorization (PMF) model coupled with self-organizing map (SOM). Environ Geochem Health 45(8):6353–6370
44. Zhang X, Wei S, Sun Q, Wadood SA, Guo B (2018) Source identification and Spatial distribution of arsenic and heavy metals in agricultural soil around Hunan industrial estate by positive matrix factorization model, principal components analysis and geo statistical analysis. Ecotoxicol Environ Saf 159:354–362
45. Cheng W, Lei S, Bian Z, Zhao Y, Li Y, Gan Y (2020) Geographic distribution of heavy metals and identification of their sources in soils near large, open-pit coal mines using positive matrix factorization. J Hazard Mater 387:1–14
46. Rudnick RL, Gao S (2014) Composition of the continental crust. The crust (ed. R.L.Rudnick), Treatise on geochemistry (eds. H.D. Holland and K.K. Turekian), 2nd. Elsevier-Pergamon, Oxford
47. Maina DM, Ndirangu DM, Mangala MM, Boman J, Shepherd K, Gatari MJ (2016) Environmental implications of high metal content in soils of a titanium mining zone in Kenya. Environ Sci Pollut Res 23:21431–21440
48. Hernandez H, Rodriguez R (2012) Geochemical evidence for the origin of vanadium in an urban environment. Environ Monit Assess 184:5327–5342
49. Chung JY, Yu SD, Hong YS (2014) Environmental source of arsenic exposure. J Prev Med Public Health 47(5):253–257
50. Bird G (2011) Provenancing anthropogenic Pb within the fluvial environment: developments and challenges in the use of Pb isotopes. Environ Int 37(4):802–819
51. Ma Y, Hooda PS (2010) Chromium, nickel and cobalt. Trace elements in soils, pp. 461–479
52. Haque MA, Subramanian V, Gibbs RJ (1982) Copper, lead, and zinc pollution of soil environment. Crit Rev Env Sci Tec 12(1):13–68
53. Thakur R, Sharma GD, Dwivedi BS, Khatik SK (2007) Chromium: as a pollutant. J Ind Pollut Control 23(2):197–203
54. Xu SA, Yu C, Wang Q, Liao J, Liu C, Huang L, Liu Q, Wen Z, Feng Y (2022) Chromium contamination and health risk

assessment of soil and agricultural products in a rural area in Southern China. Toxics 11(1):1–15
55. Alengebawy A, Abdelkhalek ST, Qureshi SR, Wang MQ (2021) Heavy metals and pesticides toxicity in agricultural soil and plants: ecological risks and human health implications. Toxics 9:1–33
56. USEPA (United States Environmental Protection Agency) (2024) Updated Dermal Exposure Assessment Guidance. Region 3 Technical Guidance Manual, Risk Assessment. Web page: https://www.epa.gov/risk/updated-dermal-exposure-assessment-guidance